Mechanical, Thermal, and Electrical Properties of Flexible Polythiophene with Disiloxane Side Chains

Shen, Jian ; Fujita, Keisuke ; Matsumoto, Takuya ; Hongo, Chizuru ; Misaki, Masahiro ; Ishida, Kenji ; Mori, Atsunori ; Nishino, Takashi

(Citation)
Macromolecular Chemistry and Physics,218(19):1700197-1700197

(Issue Date)
2017-10

(Resource Type)
journal article

(Version)
Accepted Manuscript

DOI: 10.1002/marc.

Article Type (Communication)

Mechanical, thermal and electrical properties of flexible polythiophene with disiloxane side chains

Jian SHEN, Keisuke FUJITA, Takuya MATSUMOTO, Chizuru HONGO, Masahiro MISAKI, Kenji ISHIDA, Atsunori MORI and Takashi NISHINO*

Jian SHEN, Keisuke FUJITA, Takuya MATSUMOTO, Chizuru HONGO, Kenji ISHIDA, Atsunori MORI and Takashi NISHINO*
Department of Chemical Science and Engineering,
Graduate School of Engineering, Kobe University,
Rokko, Nada, Kobe 657-8501, Japan
E-mail: tnishino@kobe-u.ac.jp

Masahiro MISAKI
Department of Comprehensive Engineering Electrical and Electronic, Kindai University Technical College, 7-1, Kasugaoka Nabari, Mie, 518-0459 Japan

---

Abstract

Poly(3-hexylthiophene) (P3HT) has been widely shown to have considerable advantages in photovoltaic cells, including excellent electrical performance, but its fragility remains a challenge for material applications and processing of stretchable devices. Herein, we synthesized high-molecular-weight and highly regioregular poly(3-substituted thiophene) with disiloxane moieties in the side chains (P3SiT). An investigation of the molecular structure and physical properties of self-supported cast films of P3SiT revealed excellent flexible mechanical properties derived from the disiloxane groups in the side chains. The larger fracture strain reached over 200% compared with that of poly(3-hexylthiophene) (14%). In addition, its Young's modulus (43 MPa) and low glass transition temperature (−10 °C) resulted in a typical elastic mechanical property. For the electrical property, the sheet resistivity of the drawn thiophene polymer showed the value almost equal to that of poly(3-hexylthiophene). The anisotropy of electrical resistivity was observed due to orientation of the drawn polymer.

FIGURE FOR ToC_ABSTRACT

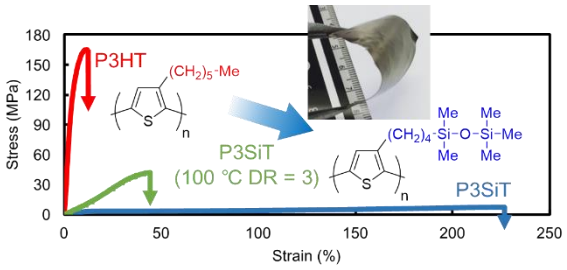

1. Introduction

Conjugated polymers have great potential in the wide field of device applications, due to the mechanical flexibility, low cost, and light weight of polymer materials.[1-3] Regioregular poly(3-alkylthiophene)s (P3ATs) with π-conjugation systems in their main chains have been focused on as notable semiconducting polymers because of their extraordinary high electrical performance. Moreover, low-cost manufacturing processes for electrical and optical devices have been developed in recent years using such materials.[4,5] Extensive investigations of P3ATs, which are one of the "element-block" polymers,[6] have revealed that their structures and properties can be changed using various chemical synthetic processes.[7-9] In particular, from the viewpoint of the chemical structure of P3ATs, long alkyl side chains always indicate environmental stability and high solubility in common organic solvents.[5] After Rieke[10] and McCullough[11] first synthesized the highly regioregular poly(3-hexylthiophene) (P3HT), it has soon been reported on the high crystallinity, high hole mobility, low band gap and high optical absorbance with the range up to 650 nm.[12] Owing to their excellent electrical properties, various polythiophene derivatives have been widely examined and have enhanced the development of organic solar cells and field-effect transistors. A number of electrical properties, such as power conversion efficiencies and charge mobilities of P3HT systems have been reported. In particular, organic solar cells with efficiencies of nearly 7% have been achieved in recent years.[13]

For widespread application in industrial fields, the mechanical properties and processability of a material are considered to be equally important to their electrical properties for the fabrication of semi-conductive polymer-based devices. However, fragile mechanical property has been one of the challenging problems of polythiophene products such as P3HT,[14] which has greatly limited the scope of industrial applications. The flexibility and bendability of P3HT are not sufficient to tolerate sequential times of multiple bending processes. Moreover, the electrical properties of P3HT decrease drastically after bending of their devices.[15] From the

viewpoint of the required mechanical performance in the application to the stretchable and wearable organic solar cells, field-effect transistors or light-emitting diodes,[16] P3HT has never been an optimal material. As it is reported that organic semi-conductors exhibit a wide range of tensile modulus, from 30 MPa to 16 GPa,[17] some of semi-conducting polymers are likely to perform more as rubbers rather than as plastics. Since the properties of P3ATs are drastically affected by the side chains on thiophene rings,[18] it is considered that the introduction of groups that are longer and more flexible than hexyl hydrocarbon groups into the side chains would lead the enhancement of flexibility of polythiophene derivatives without the loss of the electronic performance.

In this work, we synthesized a polythiophene derivative with disiloxane moieties in the side chains attached to thiophene rings (P3SiT) as shown in Figure 1 and investigated its mechanical and electrical properties. The Si–O bond distance in disiloxane in the side chains (1.66 Å)[19] is longer than the C–C bonding distance in hydrocarbon side chains (1.54 Å). Moreover, the low rotation barrier of Si–O–Si bonding (3.3 kJ/mol)[20] is comparable to the free rotation energy. These features of the disiloxane groups contribute great flexibility from the view of mechanical performance. Additionally, it is well known that conjugated polymers with higher molecular weights have better flexibility and achieve increased elongation at break.[21,22] Therefore, we synthesized a polythiophene with higher molecular weight and prepared self-supported cast films, so that the desired mechanical properties were available. Owing to the introduction of disiloxane moiety, the dissolubility and processability of polymer are particularly improved and easily dissolved in organic solvent like hexane or tetrahydrofuran.[23-27]

(Figure 1.)

2. Results and Discussion

High molecular weight and highly regioregular poly(3-substituted thiophene) with disiloxane moieties (P3SiT) was polymerized by Kumada coupling based on a nickel(II) catalyst (see Supporting Information for details of the polymerization process).[28,29] Synthesized P3SiT had a weight-average molecular weight (M_w) of 300k estimated by gel permeation chromatography (GPC), and a head-to-tail structure of over 99% was confirmed by ^{1}H NMR (see Figure S2 in the Supporting Information). After casting from hexane solution and drying for 48 hours at room temperature, the physical properties of P3SiT film were examined and compared with the high molecular weight P3HT film made by the same process. Both of the cast films are measured to be approximately same size of 50 mm × 50 mm, and the thickness of 50 μm. In the cast films of P3SiT with lower molecular weight (M_w = 60k or 130k), cracks or roughness was observed.

(Figure 2.)

The X-ray diffraction profiles (Figure 2) showed sharp peaks corresponding to the 100, which indicated highly crystalline of both synthesized P3SiT and P3HT. The diffraction angles 2θ of 100 were 4.31° for P3SiT and 2θ = 5.32° for P3HT, respectively. The 100 reflection of P3HT was observed at the same position as in previous reports.[30] The lattice spacing for the (100) (d_{100}) of P3SiT were estimated to be 20.6 Å, which was noticeably longer than that of P3HT (d_{100} = 16.6 Å). The 100 plane is defined as the distance between their main chains along the side chains. As the length of the C–Si–O–Si–Me moiety corresponds to that of four C–C bonds, the side chains of P3SiT are longer than the hexyl side chains of P3HT. In fact, the total side chain length of P3SiT is more similar to poly(3-octylthiophene) (P3OT), which has long octyl chains on thiophene rings, and fascinatingly the lattice spacing of P3SiT and P3OT indicated numerical similarity (d_{100} = 20.9 Å for P3OT).[31] The longer intermolecular distance suggests that the intermolecular interaction of P3SiT might be weaker than that of P3HT.

Additionally, the thermal properties of the obtained polymers were examined by Differential scanning calorimetry (DSC) analysis. In DSC thermograms of P3SiT and P3HT (see Figure S3 in the Supporting Information), both polymers indicate two distinct peaks corresponding to melting (T_m) and crystallization (T_c) during heating and cooling, respectively. T_m of P3SiT was observed as one endotherm peak at 142 °C, and the temperature was lower than that of P3HT at 255 °C. This difference of T_m was attributed to the weaker intermolecular interactions in P3SiT, originating from disiloxane side chains. The free volume of disiloxane side chains may lead to a decrease of the enthalpy of fusion.

(Figure 3.)

Dynamic mechanical analysis (DMA) was performed on itk DVA-200 instrument in tensile mode, and the storage modulus, loss modulus and mechanical tanδ of samples were determined as a function of temperature. Polymer cast films were at first placed in a PTFE petri dish in the heating oven and the temperature was then raised to 160 °C. After 30 min, the cast film was immediately quenched into cold water, dried up and cut into 30 mm × 5 mm for DMA. The temperature dependence (−150 °C to 100 °C) of storage modulus (E') and mechanical loss tangent (tanδ) results for P3SiT were investigated, as shown in Figure 3. In the tanδ curve, two distinct peaks at different temperatures were observed. At the lower temperature (−110 °C), a secondary transition that involves a small change in modulus was observed, which is probably attributable to motions of the polymer side chain groups,[32] namely, the behavior of disiloxane groups in P3SiT side chains. The peak at higher temperature (−10 °C), which was resulted from a primary transition involving a large change in modulus, corresponded to the glass transition temperature (T_g) of P3SiT. A huge difference was found between T_g of P3SiT and P3HT (T_g = 45 °C), and this T_g of P3SiT below ambient temperature means that P3SiT at room temperature is in a rubbery state, as shown in Table 1. The weaker intermolecular interactions and flexible

disiloxane side chains of P3SiT induced more amount of free volume, which allows this polymer to maintain the rubbery state, even at room temperature.

(Figure 4.)

Figure 4 shows X-ray diffraction photographs of undrawn and three-times-drawn (100 °C) P3SiT. Data was collected for both of the samples at various angles: “through”, “edge” and “end”. “Through” photograph means the one taken by the X-ray being irradiated from perpendicular to the cast film surface. “Edge” X-ray diffraction photographs were taken by irradiation of the X-ray beam from parallel with the surfaces and perpendicular to the drawn direction. For taking “end” photographs, the X-ray beams were irradiated from the direction parallel to drawing. In the undrawn P3SiT film, the end and edge photographs are similar owing to isotropy in the direction parallel to the surface.

The Debye–Scherrer rings were observed both in through and edge photographs of undrawn P3SiT. After drawing three times at 100 °C, several streak diffractions were clearly observed in the through and edge on photographs of drawn P3SiT, but not in the end photograph. This finding indicates that the microcrystallites of this polymer were oriented by drawing process.

(Figure 5.)

(Table 1.)

The stress–strain curves of P3SiT and P3HT cast films, as measured by tensile test, are shown in Figure 5. The P3HT film exhibited strong mechanical performance, with high tensile strength (σ_{max} = 165 MPa) and high Young’s modulus (E = 3.3 GPa). In the film of P3HT with high molecular weight and highly regioregular structure, the tensile fracture occurred immediately after loading, and the low elongation at break (ε_{max}) was low (14%). In contrast, for P3SiT with

the flexible disiloxane moieties into the side chains, the σ_{max} was decreased drastically (6 MPa), but the ε_{max} (226%) was approximately 20 times higher than that of P3HT (Table 1). The synthesized polythiophene P3SiT, which was in a rubbery state at ambient temperature because of the weak intermolecular interaction and the disiloxane moieties, showed a great increase in flexibility relative to P3HT. In contrast, three-times-drawn P3SiT had Young's modulus of E = 129 MPa and tensile strength of σ_{max} = 42 MPa, which were two and seven times higher than those of undrawn P3SiT, respectively, owing to increased orientation and crystallinity following the drawing processes. These increases imply that the mechanical performance of P3SiT could be controllable by hot drawing. For investigation of the elastomeric performance of P3SiT, we also carried out repeated loading–unloading tensile tests. The stress–strain curves of P3SiT at different tensile strains during loading–unloading tests are described in the Supporting Information. Below 10% of the tensile strain, the P3SiT film demonstrated high elastic recovery. As the strain was increased above 10%, the permanent deformation occurred in the P3SiT film, and it finally lost the elastic recovery when the tensile strain was up to 50%. For the achievement of the high elasticity and recovery in polythiophene derivatives, the one of the best way should be the introduction of the physical or chemical crosslinking to this P3SiT.

The current–voltage curves of P3HT and P3SiT, and those of three-times-drawn P3SiT collected parallel and perpendicular to the drawn direction were collected using the four-terminal sensing method (see Figure S6 in the Supporting Information). The electrical resistivity (R) of these samples as function of voltage were calculated using Ohm's law. We chose to use the average value in the region where the electrical resistivity levels off for these samples. The electrical resistivity (R) and sheet resistivity (R_s) of the samples are summarized in Table 2. Owing to the larger and longer side chains of P3SiT, the sheet resistivity (1.8×10^6 Ω / square) was larger value than that of P3HT (1.3×10^6 Ω / square). It has been reported by several groups that the electrical performance of P3ATs, such as charge mobility in field-effect transistors, is deleteriously affected by increasing the length of side chains.[33,34] In addition,

from the electrical measurements in the two different directions of drawn P3SiT samples, we observed high anisotropy of sheet resistivity (see also in Table 2). The sheet resistivity of drawn P3SiT parallel to the drawn direction was much lower than that perpendicular to the drawn direction, nearly half in value. The absolute value in the parallel direction (1.1×10^6 Ω / square) was comparable to that of P3HT. These results indicate that the electrical resistivity of polythiophene derivatives is controllable by hot drawing.

(Table 2.)

3. Conclusions

In summary, we synthesized high molecular weight (M_w = 300k) and highly regioregular (> 99 %) poly(3-substituted thiophene) with disiloxane moieties, and investigated the molecular structure and mechanical, thermal and electrical properties. The identified sharp peak in the X-ray diffraction profile and the observation of melting endotherm and crystallization exotherm peaks by DSC indicated that this polymer has highly crystalline. Owing to the flexible disiloxane groups in the side chain of thiophene rings, the glass transition temperature of the polymer (−10 °C) was much lower than ambient temperature. As we expected, the synthesized polymer exhibited high mechanical flexibility and showed low tensile strength (6 MPa), but over 200% elongation at break. Moreover, after drawing of P3SiT, the tensile strength and modulus were increased. Measurements of the electrical performance indicated that the disiloxane side chains made it relatively higher electrical resistance of undrawn P3SiT compared with that of P3HT. The drawing process introduced electrical anisotropy into drawn P3SiT, with electrical resistivity comparable to that of P3HT in the direction parallel to drawing.

Supporting Information

Supporting Information is available from the Wiley Online Library.

Appendix/Nomenclature/Abbreviations

Acknowledgements: This work was supported by a Grant-in-Aid for Scientific Research on Innovative Areas “New Polymeric Materials Based on Element-Blocks (No.2401)” (24102009) of The Ministry of Education, Culture, Sports, Science, and Technology, Japan. The synchrotron radiation experiments were performed at the BL03XU of SPring-8 with the approval of the Japan Synchrotron Radiation Research Institute (JASRI) (Proposal No. 2015A7210, 2015B7260, 2016A7210, and 2016B7260).

Keywords: polythiophene; high molecular weight; high elasticity; conductive polymer; conjugated polymer.

References

[1] W. Lu, *Science* **2002**, *297*(5583), 983–987.

[2] E. W. H. Jager, *Science* **2000**, *290* (5496), 1540–1545.

[3] T. D. Nguyen, G. Hukic-Markosian, F. Wang, L. Wojcik, X. G. Li, E. Ehrenfreund, Z. V. Vardeny, *Nat. Mater.* **2010**, *9*, 345–352.

[4] G. Horowitz, *Adv. Mater.* **1998**, *10*, 365–377.

[5] S. Samitsu, T. Shimomura, S. Heike, T. Hashizume, K. Ito, *Macromolecules* **2008**, *41*, 8000–8010.

[6] Y. Chujo, K. Tanaka, *Bull. Chem. Soc. Jpn.* **2015**, *88*, 633–643.

[7] M. J. Winokur, D. Spiegel, Y. Kim, S. Hotta, A. J. Heeger, *Synth. Met.* **1989**, *28*, 419–426.

[8] G. Zerbi, B. Chierichetti, O. Ingänas, *J. Chem. Phys.* **1991**, *94*, 4637–4645.

[9] S. Savagatrup, A. D. Printz, D. Rodriquez, D. J. Lipomi, *Macromolecules* **2014**, *47*, 1981–1992.

[10] T. Chen, R. D. Rieke, *J. Am. Chem. Soc.* **1992**, *114*, 10087–10088.

[11] R. D. McCullough, S. Tristram-Nagle, S. P. Williams, R. D. Lowe, M. Jayaramn, M. Jayaraman, M. Jayaramn, M. Jayaraman, *J. Am. Chem. Soc.* **1993**, *115*, 4910–4911.

[12] M. T. Dang, L. Hirsch, G. Wantz, J. D. Wuest, *Chem. Rev.* **2013**, *113*, 3734–3765.

[13] R. Ganesamoorthy, G. Sathiyan, P. Sakthivel, *Sol. Energy Mater. Sol. Cells* **2017**, *161*, 102–148.

[14] J. S. Kim, J. H. Kim, W. Lee, H. Yu, H. J. Kim, I. Song, M. Shin, J. H. Oh, U. Jeong, T. S. Kim, B. J. Kim, *Macromolecules* **2015**, *48*, 4339–4346.

[15] T. F. O'Connor, A. V. Zaretski, S. Savagatrup, A. D. Printz, C. D. Wilkes, M. I. Diaz, E. J. Sawyer, D. J. Lipomi, *Sol. Energy Mater. Sol. Cells* **2016**, *144*, 438–444.

[16] J. Y. Oh, S. Rondeau-Gagné, Y. C. Chiu, A. Chortos, F. Lissel, G. J. Nathan Wang, B. C. Schroeder, T. Kurosawa, J. Lopez, T. Katsumata, J. Xu, C. Zhu, X. Gu, W. G. Bae, Y. Kim, L. Jin, J. W. Chung, J. B. H. Tok, Z. Bao, *Nature.* **2016**, *539*, 411–415.

[17] D. Tank, H. H. Lee, D. Y. Khang, *Macromolecules* **2009**, *42*, 7079–7083.

[18] M. Sundberg, O. Inganäs, S. Stafström, G. Gustafsson, B. Sjögren, *Solid State Commun.* **1989**, *71*, 435–439.

[19] F. Bauer, S. Czihal, M. Bertmer, U. Decker, S. Naumov, S. Wassersleben, D. Enke, *Microporous Mesoporous Mater.* **2015**, 1–11.

[20] A. Colas, *Silicones: Preparation, Properties and Performance*, Dow Corning, Life Sciences, **2014**, available at: http://www.dowcorning.com/content/publishedlit/01-3077.pdf (accessed February 2014).

[21] B. Deffner, A. D. Schlüter, *Polymer Chemistry* **2002**, *6*, 7833–7840.

[22] B. Deffner, S. Jimaja, A Kroeger, A. D. Schlüter *Macromol. Chem. Phys.* **2017**, *218*, 1600561.

[23] M. Funahashi, A. Sonoda, *Org. Electron. physics, Mater. Appl.* **2012**, *13*, 1633–1640.

[24] J. Lee, A. Han, J. Kim, Y. Kim, J. H. Oh, C. Yang, *J. Am. Chem. Soc.* **2012**, *134*, 20713–20721.

[25] J. Lee, A. Han, H. Yu, T. J. Shin, C. Yang, J. H. Oh, *J. Am. Chem. Soc.* **2013**, *135*, 9540–9547.

[26] A. Han, J. Lee, H. R. Lee, J. Lee, S. Kang, H. Ahn, T. J. Shin, J. H. Oh, C. Yang, *Macromolecules* **2016**, *49*, 3739–3748.

[27] E. K. Lee, C. H. Park, J. Lee, H. R. Lee, C. Yang, J. H. Oh *Adv. Mater.* **2017**, *29*, 1605282.

[28] X. Hu, *Chem. Sci.* **2011**, *2*, 1867–1886.

[29] K. Fujita, Y. Sumino, K. Ide, S. Tamba, K. Shono, J. Shen, T. Nishino, A. Mori, T. Yasuda, *Macromolecules* **2016**, *49*, 1259–1269.

[30] Y. S. Kim, Y. Lee, J. K. Kim, E. O. Seo, E. W. Lee, W. Lee, S. H. Han, S. H. Lee, *Curr. Appl. Phys.* **2010**, *10*, 985–989.

[31] S. Malik, A. K. Nandi, *J. Polym. Sci. Part B Polym. Phys.* **2002**, *40*, 2073–2085.

[32] I. M. Ward, *Mechanical Properties of Solid Polymers*, John Wiley & Sons, **2012**, p. 138.

[33] S. T. Salammal, E. Mikayelyan, S. Grigorian, U. Pietsch, N. Koenen, U. Scherf, N. Kayunkid, M. Brinkmann, *Macromolecules* **2012**, *45*, 5575–5585.

[34] A. Babel, S. A. Jenekhe, *Synth. Met.* **2005**, *148*, 169–173.

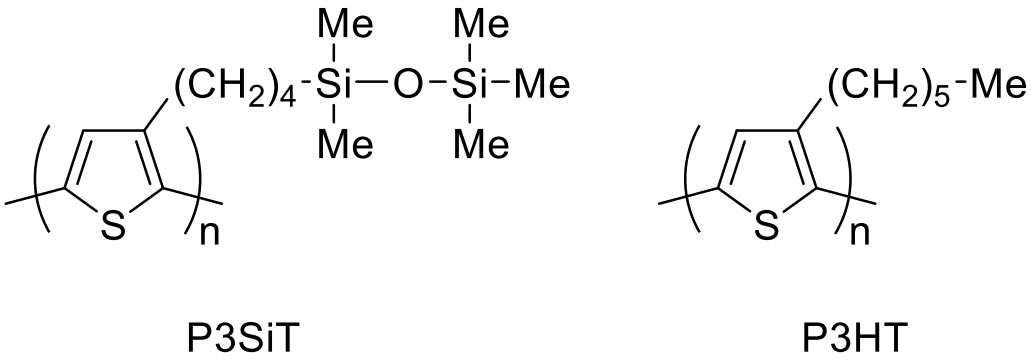

P3SiT P3HT

Figure 1. Chemical structure of poly(3-substituted thiophene) with disiloxane moieties (P3SiT)(left) and poly(3-hexylthiophene)(P3HT)(right).

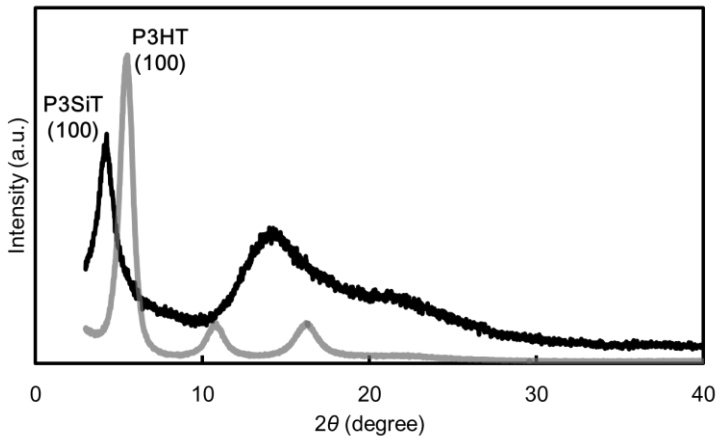

Figure 2. X-ray diffraction profiles of P3SiT and P3HT.

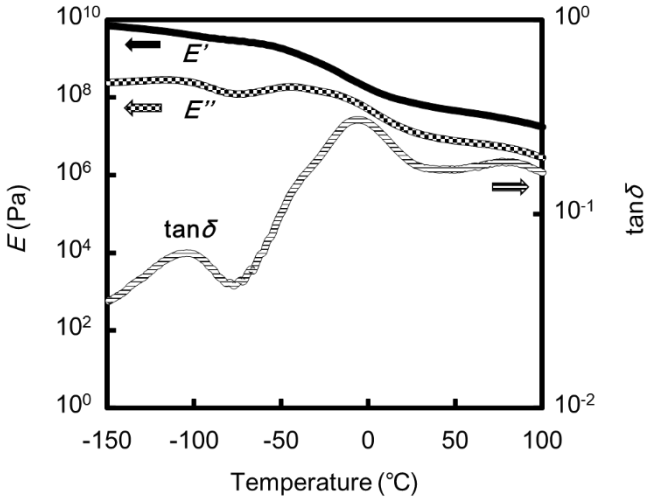

Figure 3. Temperature dependence of storage modulus (*E'*), loss modulus (*E"*) and tanδ of P3SiT measured by dynamic mechanical analysis (DMA).

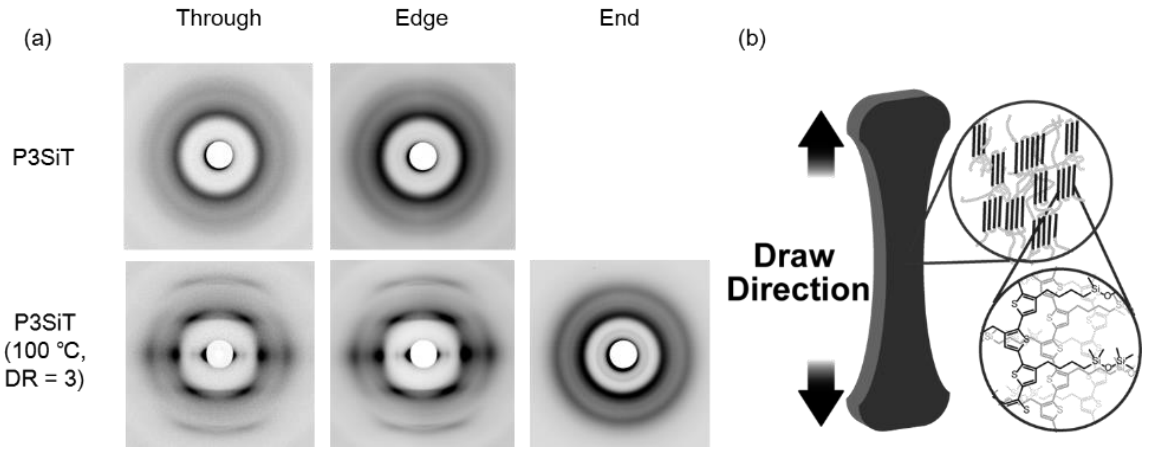

Figure 4. (a) X-ray diffraction photographs of P3SiT and three-times-drawn (100 °C) P3SiT. Photographs of P3SiT sample are taken by through and edge direction to cast film surface, three-times drawn (100 °C) P3SiT are taken by through, edge and end direction to cast film surface respectively. (b) Schematic model of microstructure of drawn P3SiT.

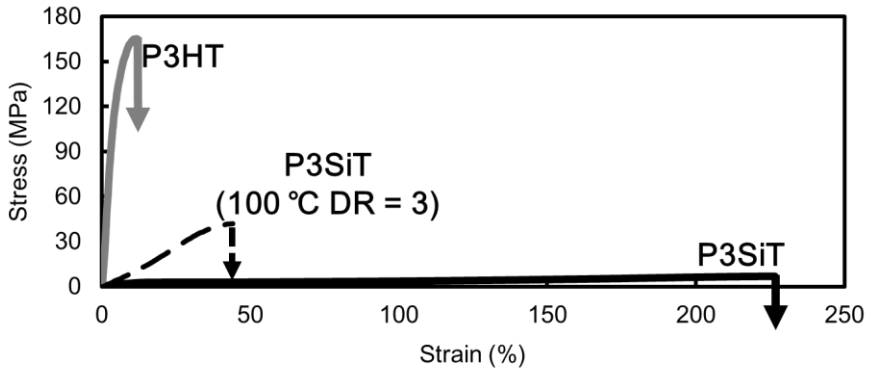

Figure 5. Stress-strain curves of P3HT, P3SiT and three-times-drawn P3SiT at 100 °C measured by tensile testing.

Table 1. Machanical and thermal properties of P3SiT, P3HT and three-times-drawn P3SiT at 100 °C measured by tensile testing. (E : Young's modulus, σ_{max} : tensile strength, ε_{max} : fracture strain, T_g : glass transition temperatur, T_m : melting temperature and T_{d5} : melting decomposition temperature)

Polymer	E (MPa)	σ_{max} (MPa)	ε_{max} (%)	T_g (°C)	T_m (°C)	T_{d5} (°C)
P3SiT	43 (±8)	6 (±0.4)	226 (±8.6)	−10	142	420
P3HT	3300 (±320)	165 (± 37)	14 (±2.4)	45	255	380
P3SiT (100°C DR = 3)	129 (±54)	42 (± 11)	44 (±8.9)	–[a]	141	405

[a] Samples were broken at low temperature.

Table 2. Electrical resistivity and sheet resistivity of P3SiT, P3HT, the parallel direction and the perpendicular direction of three-times-drawn P3SiT cast films measured by four-terminal sensing method.

Polymer	R (Ω)	R_s (Ω / square)
P3SiT	6.2×10^4	1.8×10^4
P3HT	4.6×10^4	1.3×10^4
P3SiT (100°C DR = 3) perpendicular	7.3×10^4	2.1×10^4
P3SiT (100°C DR = 3) parallel	4.0×10^4	1.1×10^4

ToC figure

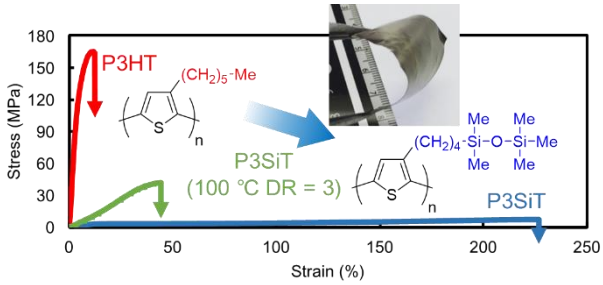
180
150
120
90
60
30
0
Stress (MPa)
0
50
100
150
200
250
Strain (%)
P3HT
(CH2)5-Me
S
n
P3SiT
(100 °C DR = 3)
(CH2)4-Si-O-Si-Me
Me
Me
Me
Me
P3SiT